LWT - Food Science and Technology 165 (2022) 113704

Contents lists available at ScienceDirect

LWT

journal homepage: www.elsevier.com/locate/lwt

Linking the yield stress functionality of polyglycerol polyricinoleate in a highly filled suspension to its molecular properties

Ruth Price [a,*], David Gray [a], Nicholas Watson [b], Josélio Vieira [c], Bettina Wolf [d,**]

[a] Division of Food, Nutrition and Dietetics, School of Biosciences, University of Nottingham, Sutton Bonington Campus, Loughborough, Leicestershire, LE12 5RD, United Kingdom
[b] Food, Water, Waste Research Group, Faculty of Engineering, University of Nottingham, Nottingham, NG7 2RD, United Kingdom
[c] Nestlé Product Technology Centre, Haxby Road, PO Box 204, York, YO91 1XY, United Kingdom
[d] School of Chemical Engineering, University of Birmingham, Birmingham, B15 2TT, United Kingdom

ARTICLE INFO

Keywords:
PGPR
Sugar-in-oil suspensions
Chocolate rheology
Molecular weight
Estolide

ABSTRACT

Polyglycerol polyricinoleate (PGPR) is a food emulsifier with a unique yield stress reducing efficacy in fat-based suspensions. There are many commercially available PGPRs, and the different products vary in their impact on the yield stress. Choosing the right PGPR for a specific formulation is often based on empirical data and the experience of the formulator. Lack of fundamental understanding of why these differences exist hampers reformulation efforts to replace PGPR. Therefore, this study aimed to link the yield stress reducing efficacy of PGPR to its molecular properties. Five commercial PGPR samples were studied (3 g/kg) in a concentrated suspension of icing sugar (650 g/kg, ≈ 530 mL/L) in sunflower oil (with naturally-occurring surface-active molecules removed). Rheological analysis revealed Herschel-Bulkley yield stress variations of between 0.90 ± 0.06 Pa and 1.90 ± 0.18 Pa, compared to 57.6 ± 15.8 Pa in the absence of PGPR. Yield stress was correlated to critical micelle concentration, obtained from oil-water interfacial tension data. Applying molecular characterisation techniques revealed that the presence of a hydroxyl group on the fatty acid at the end of the polyricinoleate estolide chain could be linked to inferior yield stress reducing efficacy.

1. Introduction

Chocolate is a composite material of particles of sugar, cocoa mass and sometimes milk powder dispersed in a crystallised fat phase, composed mainly of cocoa butter but may contain small amounts of other fats and emulsifiers. Upon melting, the solid composite transforms into a concentrated fat-based suspension. As with many suspensions, the rheology of chocolate is often described in terms of its yield stress and viscosity (Beckett, 2019). Emulsifiers are added to increase the wettability of the dispersed particles and aid their distribution throughout the continuous fat phase (Johansson & Bergenståhl, 1992a), affecting the rheological properties which are important both in processing (Gonçalves & Lannes, 2010) and mouthfeel perception (Kamphuis, 2017; Ziegler & Hogg, 2017). Polyglycerol polyricinoleate (E476, PGPR) is unique among food emulsifiers for having a substantial effect on the yield stress of fat-based suspensions. Adding just 1 g/kg of PGPR to a chocolate formulation causes a yield stress reduction equivalent to 30 g/kg of extra cocoa butter, reducing the inclusion of this expensive and calorific ingredient (Rector, 2000). If PGPR is added at 10 g/kg, the yield value becomes zero (Bamford, Gardner, Howat, & Thomson, 1970). The method by which PGPR reduces the yield stress at the molecular level has not been fully ascertained. As with other emulsifiers, the hydrophilic headgroup likely adsorbs at the sugar surface, and its yield stress reduction functionality may merely be due to its long hydrophobic chains providing an extended steric barrier (Vernier, 1997). However, using scanning electron microscopy, “pillow-like deposits” have been

Abbreviations: CMC, critical micelle concentration; ESI-MS, electrospray ionisation-mass spectroscopy; FAME, fatty acid methyl ester; GC-MS, gas chromatography-mass spectroscopy; H–B, Herschel-Bulkley; MWR, molecular weight range; NMR, nuclear magnetic resonance; PG, number of glycerol units in the polyglycerol chain; PGPR, polyglycerol polyricinoleate; PMMA, poly(methyl methacrylate); PR, number of fatty acid units in the polyricinoleate chain; SEC, size-exclusion chromatography; TAG, triacylglycerol; TMSH, trimethylsulfonium hydroxide.

* Corresponding author.
** Corresponding author.
E-mail addresses: ruth.price1@nottingham.ac.uk (R. Price), david.gray@nottingham.ac.uk (D. Gray), nicholas.watson@nottingham.ac.uk (N. Watson), Joselio.Vieira@rdyo.nestle.com (J. Vieira), b.wolf@bham.ac.uk (B. Wolf).

https://doi.org/10.1016/j.lwt.2022.113704
Received 17 January 2022; Received in revised form 16 June 2022; Accepted 23 June 2022
Available online 27 June 2022

observed on the surface of sugar crystals suspended in cocoa butter containing 5 g/kg PGPR. These deposits were found to be a mixture of PGPR and trapped cocoa butter triacylglycerols, and were argued to act as a buffer between the particles, preventing the formation of the attractive bonds that create the yield stress phenomenon (Middendorf, Juadjur, Bindrich, & Mischnick, 2015).

The PGPR molecule is composed of a polyglycerol headgroup esterified with one or more polyricinoleate chains, as depicted in Fig. 1 (here, two chains are shown). PGPR is synthesised from castor oil by first releasing the fatty acids from the triacylglycerols by hydrolysis. The fatty acids are purported to be 80–90% ricinoleic acid, with oleic, linoleic, and stearic acid found at 3–8%, 3–7% and 0–2%, respectively (Wilson, Van Schie, & Howes, 1998). These fatty acids are condensed into polyricinoleate estolide chains via the hydroxyl group on the ricinoleic acid. Separately, polyglycerol chains are created by condensing glycerol forming ether bonds. Finally, the polyglycerols are added to the polyricinoleates, a condensation reaction occurs, and esterification links the two groups of chains together (Wilson et al., 1998). The non-ricinoleate fatty acids obtained from the original castor oil feedstock act as caps for the chains halting the estolide formation process (Isbell, 2011; Zerkowski, 2008). This method of PGPR production results in a mixture of molecules of different molecular weights, based on different quantities of glycerol units and fatty acid units. According to Bastida-Rodríguez (2013), the average number of glycerol molecules in the polyglycerol chain is three, and the average number of fatty acids in each of the polyricinoleate chains is between five and eight. The author also postulated that a typical PGPR molecule has two polyricinoleate chains condensed at the two ends of the polyglycerol molecule. This "average" PGPR molecule, having three glycerols and two chains of five polyricinoleates, would have a molecular weight of 3054 g/mol. Orfanakis et al. (2012) measured the molecular weight range (MWR) of two PGPR samples. Using Electrospray Ionisation-Mass Spectrometry (ESI-MS), they found an average molecular weight of around 1170 g/mol and an MWR range of 400–2000 g/mol. Others cite an MWR of several hundred to over 4000 g/mol, based on size-exclusion chromatography data (Dedinaite & Campbell, 2000). For application in foods, PGPR is highly controlled by regulatory bodies, including the European Union (CEC, 2008) and the United Nations (JECFA, 1992), and the International Food Chemical Codex (FCC, 2016).

While in practice, experienced product formulators are aware of differences in the yield stress lowering performance of commercial PGPR, future developments and re-developments of emulsifiers would benefit from understanding the origin of these differences. This current work tests the hypothesis that the yield stress reducing efficacy of PGPR is linked to its molecular properties. Five commercial PGPR samples were obtained that were described by their manufacturers as a yield stress controlling product or general-purpose lipid emulsifier. Each PGPR was applied in a highly concentrated sugar-oil suspension, and the yield stress lowering capacity was quantified using rotational rheology. Since the functionality of PGPR relates to interfacial behaviour, additionally, the critical micelle concentration (CMC) and the predicted interfacial area per molecule were determined for each PGPR from the oil/water interfacial tension curves. Electrospray ionisation-mass spectroscopy (ESI-MS), size exclusion chromatography (SEC) and nuclear magnetic resonance (NMR) spectroscopy were applied as complementary methods to characterise the molecular properties of the five samples. Finally, since the fatty acid profile of the PGPRs may be important in the action of the PGPR, this was also analysed using transmethylation followed by gas chromatography-mass spectroscopy (GC-MS). The data on PGPR performance in direct comparison to its molecular properties provide potentially exploitable insights in view to identifying a natural alternative to PGPR, aligning with shifting industry trends towards clean label products (Osborn, 2015).

2. Materials and methods

2.1. Materials

Samples of five commercial polyglycerol polyricinoleate samples were kindly donated by their manufacturers and randomly coded PGPR-1 to PGPR-5 using an online app (random.org). Anonymity was chosen to remove bias and shorten figure labels; see Table S1 for the trade names.

Sunflower oil (from a local supermarket) and icing sugar (British Sugar, LCO Trading Store, Staffordshire, UK) were the formulation ingredients for the sugar-in-oil suspensions. Magnesium silicate (Florisil®, <200 mesh, fine powder, Sigma-Aldrich, Saint Louis, USA) was utilised to remove surface-active molecules from the sunflower oil (see section 2.3). Acetone (VWR Chemicals, Rosny-sous-Bois, France) was used in the ESI-MS experiments. Deuterated chloroform (Sigma-Aldrich, Saint Louis, USA) was used for NMR experiments. Methyl pentadecanoate, trimethylsulfonium hydroxide (TMSH) (Sigma-Aldrich, Saint Louis, USA) and chloroform (HPLC grade, Fisher Scientific, Loughborough, UK) were applied in the transmethylation procedure and lipid extraction.

2.2. Sunflower oil pre-treatment

The naturally present surface-active molecules in sunflower oil were removed using magnesium silicate following a published protocol (Gould, Furse, & Wolf, 2016). A mixture of 40 g/kg of the absorbent in sunflower oil was stirred for 30 min at 600 rpm and 22 ± 1 °C on a magnetic stirrer (Carousel Tech Stirring Hotplate, Radleys, Saffron Walden, UK). The magnesium silicate was then removed by centrifugation at 2700*g* and 20 °C for 30 min (Jouan CR3i multifunction Centrifuge, Thermo Fisher Scientific, Waltham USA). The treated sunflower oil was stored in amber glass bottles at 22 ± 1 °C in the dark for no more than two weeks, and the absence of surface-active molecules

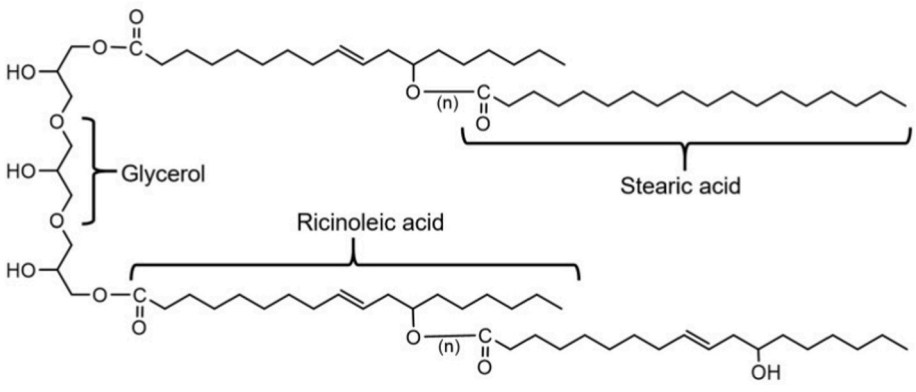

Fig. 1. Molecular structure of polyglycerol polyricinoleate (PGPR). The polyglycerol chain shown is formed from three glycerol units; however, the polyglycerol in PGPR can have more or fewer than this. The polyricinoleate chain includes "n", which indicates that several ricinoleic acids can be included in this chain. A PGPR molecule can have one polyricinoleate chain, two (as shown here) or more – the limit is the number of hydroxyl groups to react with and the geometry of the molecule. The structure also illustrates that the terminal fatty acid on the polyricinoleate chain can be a ricinoleic acid (as shown on the bottom chain) or another fatty acid (as shown on the top chain). Stearic acid is shown here as the terminal fatty acid; however, other fatty acids have been found in castor oil.

was validated at least every three days through interfacial tension measurement, see section 2.6.

2.3. Sugar pre-treatment and particle size

The icing sugar was dried overnight in batches of around 100 g in a vacuum oven (Gallenkamp, Fistreem International, Cambridge, UK), 80 kPa at 60 °C and then left to cool in a desiccator at room temperature (22 ± 1 °C).

Sugar particle size distributions were acquired using laser diffraction equipment (Mastersizer 2000, Malvern Instruments Ltd, Malvern, UK). The icing sugar was dispersed by manual stirring in sunflower oil containing 5 g/kg PGPR-5. The dispersion was sonicated and then applied to the liquid dispersion cell of the instrument. The volume-weighted mean particle size was 35 μm, and 90% of the particles (by volume) were smaller than 87 μm.

2.4. Sugar-in-oil suspensions

Sugar-in-oil suspensions composed of 650 g/kg dried icing sugar, 347 g/kg treated sunflower oil and 3 g/kg PGPR were prepared, as follows. Initially, PGPR was added to treated oil and stirred for 60 min at 100 rpm and 22 ± 1 °C using a magnetic stirrer. Dried icing sugar was then combined with the oil phase at an equal weight basis, manually stirred with a spatula until all sugar particles appeared to have been wetted by the oil phase, followed by mixing with a high shear overhead mixer (SilversonL5M, Silverson Machines Ltd, Chesham, UK) for 4 min at 8000 rpm. The sample batch size was kept constant at 190 g and contained in a 250 mL glass beaker in an ice bath, keeping the mixture's temperature below 47 °C to avoid the risk of oxidation (Crapiste, Brevedan, & Carelli, 1999). Prepared suspensions were stored for 39 ± 2 h at 22 ± 1 °C, away from light, before adjusting the solid phase fraction to 650 g/kg by centrifugation (Beckman Model J2-21 centrifuge, with JA-14 fixed angle motor, Beckman Coulter (UK) Ltd., High Wycombe, UK) for 10 min at 3836 g and 10 °C followed by the removal of the appropriate amount of supernatant to obtain a final suspension with a solid phase fraction of 650 g/kg or ≈ 530 mL/L. The sample was manually stirred with a spatula and then left to stand for at least 10 min before applying to the rheometer. Reference suspensions were prepared following the same protocol except for the addition of PGPR. All samples were prepared in duplicate.

2.5. Yield stress

Sugar-in-oil suspension yield stress data were obtained from unidirectional stress ramp data acquired on a stress-controlled rheometer (MCR 301, Anton Paar, Graz, Austria) fitted with a serrated cup (inner diameter: 28.92 mm) and serrated bob (outer diameter: 26.66 mm; length: 40.00 mm) geometry. Measurement temperature was 20 °C as previously used (Johansson & Bergenståhl, 1992b), controlled by a Peltier system. The sample was manually applied to the geometry, and the measurement started immediately. The rheological protocol consisted of a stepwise decrease in shear stress from 1000 Pa to 0.1 Pa, collecting ten logarithmically spaced data points per decade. Each stress was applied for 10 s, and then the data was collected. The results are graphed as relative viscosity (Equation (1)) versus shear stress to visualise the change in suspension viscosity upon the addition of PGPR. Finally, utilising the rheometer's software package (Anton Paar RheoPlus), the data were fitted to the Herschel-Bulkley model (Equation (2)) to obtain the Herschel-Bulkley (H–B) yield stress value.

$$\eta_{rel}(Pa) = \frac{\eta_{susp}(Pa)}{\eta_m} \tag{1}$$

where η_{rel} (1) is the relative viscosity, τ (Pa) the shear stress, η_{susp} (Pa.s) the viscosity of the sugar-in-oil suspension, and η_m (Pa.s) the viscosity of the continuous suspension phase. η_m was constant over the τ range of measurement. The viscosity of treated sunflower oil was 62.8 mPa s (±0.12 mPa s, n = 3) and the effect of adding PGPR reduced this slightly, but significantly ($t_{(4)} = 45.7$, $p < 0.01$), to 61.0 mPa s (±0.18 mPa s, n = 3). Therefore, using relative viscosity meant that the impact of the different continuous phase viscosity was negated.

$$\tau = \tau_{H-B} + k(\dot{\gamma})^n \tag{2}$$

where τ (Pa) is the shear stress, τ_{H-B} (Pa) the Herschel-Bulkley (H–B) yield stress, k (Pa.s^n) the consistency index, $\dot{\gamma}$ (1/s) the shear rate, and n (1) the flow index. Triplicate measurements were conducted on each of the two sample batches, and the results are shown as H–B yield stress and the percentage reduction in yield stress as defined by Equation (3).

$$\text{Yield stress reduction } [\%] = \left(1 - \frac{\tau_{HB}}{\tau_{HB,ref}}\right) * 100\% \tag{3}$$

where $\tau_{HB,ref}$ (Pa) is the Herschel-Bulkley yield stress of the reference sample.

2.6. Interfacial property analyses

Interfacial tension data were acquired on a pendant drop tensiometer (Profile Analysis Tensiometer PAT1, SINTERFACE Technologies, Berlin, Germany) to verify the treatment of sunflower oil with magnesium silicate was successful and to characterise the interfacial activity of the PGPR samples. The treated sunflower oil ± PGPR was contained in a quartz glass cuvette kept at 20 °C using a water bath (Grant Instruments, Cambridge, UK). A drop of ultrapure water was pendant from a straight capillary (stainless steel, 2 mm outer diameter) into the oil, and the cross-sectional area was set to remain constant (25 mm^2). Drop profile images were taken every second until the interfacial tension changed by less than ±0.1 mN/m over 400 s. The average of the interfacial tension data over the last 400 s was taken as the equilibrium interfacial tension. The treatment of the sunflower oil to remove naturally occurring surface-active components was deemed a success if the interfacial tension of the oil reached equilibrium within 400 s of droplet formation. The equilibrium interfacial tension of the treated sunflower oil was 25.3 ± 1.3 mN/m.

To create the interfacial tension isotherms, PGPR was initially added to treated sunflower oil at a concentration of 50 g/kg (see section 2.4 for the dissolution protocol). From this, serial dilutions were performed down to 0.2 g/kg PGPR and kept in the dark for a maximum of 3 days at 22 ± 1 °C. Two batches of each PGPR/concentration were produced and analysed. Critical micelle concentration (CMC) values were obtained as the intercept of linear regression lines fitted to the two regions of the semi-logarithmic plot of interfacial tension versus concentration, excluding the data at the lowest concentration to improve the quality of fit of the lower concentrations close to the CMC. The slope of the regression lines in this region was then inserted into the Gibbs adsorption isotherm (Equation (4)). The obtained interfacial excess value was further transformed (Equation (5)) to calculate the projected interfacial area occupied per adsorbed PGPR molecule in Å^2.

$$\Gamma = -\frac{1}{2.303RT}\frac{d\gamma}{d\ln c} \tag{4}$$

where Γ is the interfacial excess (mol/m^2), R the gas constant (J/mol.K), T the temperature (K), $d\gamma$ the change in interfacial tension (N/m), and $d\ln c$ the change in the (ln) concentration (no units).

$$Areapermolecule = \frac{1}{\Gamma}\frac{10^{20}\text{Å}^2}{6.02*10^{23} molecules} \tag{5}$$

2.7. Electrospray ionisation-mass spectrometry

Electrospray ionisation-mass spectrometry (ESI-MS) was applied to

all PGPR samples to assess their molecular weight range (MWR). Following literature protocol with slight modification (Orfanakis et al., 2012), PGPR was initially mixed with acetone (10 g/kg); 250 μL of this was removed and mixed with 600 mL/L methanol/400 mL/L water containing 2 mL/L formic acid (50 μL). This mixture was injected into the electrospray source of a mass spectrometer (Micromass Quattro Ultima, Waters, Milford, USA) using a 250 μL glass syringe (SGE Analytical Science, Melbourne, Australia) fitted to a syringe pump (model 22, Harvard Apparatus, Holliston, USA) set at 100 μL/min. The source was in positive-ion mode, 4.2 kV capillary voltage, 25 V cone voltage, 250 °C desolvation temperature, and desolvation gas at 188 L/h. The experiments were performed at a low resolution to enable the size of the polymeric PGPR molecules to be detected. The spectra were recorded from m/z 200–3000 using MassLynx version 4.0 (Waters Corporation, Milford, USA).

2.8. Size exclusion chromatography

Size exclusion chromatography (SEC) was also used to assess the MWR of the PGPR samples. An Agilent Infinity II MDS instrument featuring differential refractive index, viscometry, dual-angle light scatter and two-wavelength UV detectors was equipped with 2 x PLgel Mixed C columns (300 × 7.5 mm) and a PLgel 5 μm guard column. The eluent was chloroform. Samples were analysed at 1 mL/min and 30 °C. Poly(methyl methacrylate) (PMMA) standards (EasiVials, Agilent, Santa Clara, USA) were used for calibration. Before injection, analytical samples were filtered through a PTFE filter (0.22 μm pore size). Molecular weight averages were determined by third-order PMMA conventional calibration (1,568,000–960 g/mol) using SEC software (Agilent Santa Clara, USA).

2.9. Nuclear magnetic resonance spectroscopy

Nuclear magnetic resonance (NMR) spectroscopy was employed to assess the length of the polyricinoleate chains of the PGPR molecules by comparing the alkene regions of the most and the least efficient PGPR sample. These PGPRs were dissolved in deuterated chloroform (1:1 by weight) and around 600 μL placed into clean NMR tubes. Spectra were then acquired at 25 °C (Avance Neo 800 MHz NMR Spectrometer, Bruker, Karlsruhe, Germany) using a 5 mm QCI Cryoprobe. A total of 128 scans of 32K points with a spectral width of 13 ppm were collected. The free induction decays were multiplied by an exponential weighting function with a line broadening of 0.3 Hz before Fourier transformation. Phasing and baseline corrections were performed, and the spectra were processed using Topspin Software (Bruker, Karlsruhe, Germany).

2.10. Gas chromatography-mass spectrometry

The fatty acid types at the end of the polyricinoleate chains of the PGPR molecules were assessed using transesterification followed by gas chromatography coupled to mass spectrometry detection (GC-MS). The PGPR samples were dissolved in chloroform (1:5 by weight), and 1 mL of dissolved lipid was measured into a clean glass bijou bottle. Methyl pentadecanoic acid (100 μL; internal standard) (Sigma-Aldrich, Darmstadt, Germany) was added, followed by 200 μL of trimethylsulfonium hydroxide (TMSH) (0.25M solution in methanol, ACROS Organics™, Geel, Belgium). The bottle was capped, vortex-mixed and left for at least 10 min to ensure the TMSH had liberated and formed salts with the fatty acids. The mixture was then filtered through a 0.45 μm PTFE filter membrane (Whatman, GE Healthcare Life Sciences, Chicago, USA) and stored in amber glass vials at −20 °C until analysis.

The TMSH reaction was completed in the injector of the GC-MS (DSQ, Thermo Fisher Scientific, Waltham, USA), and fatty acid methyl esters (FAME) were analysed using a published method (Bahrami et al., 2014) with slight modification. The samples (1 μL) were injected into a Phenomenex Zebron ZB-FFAP (30 m × 0.25 mm) column using a vaporising injector with a split flow of 50 mL/min of helium. The oven temperature was maintained at 120 °C for 1 min and then increased to 250 °C at a rate of 5 °C/min before holding for 2 min. Detection was conducted using a mass spectrometer, and individual fatty acids were identified using a mass spectrum library and comparing retention times and molecular mass to FAME standards.

2.11. Statistical analysis

Experimental data were analysed using a one-way analysis of variance (ANOVA) followed by a Tukey post-hoc test, or a Pearson product-moment correlation, using SPSS (Statistics v 27, IBM Corp, Armonk, USA), with a significance level set at $p < 0.05$. Linear regression was performed with MS Excel software.

3. Results and discussion

3.1. Yield stress reducing efficacy

Rheological data to assess the yield stress properties of commercial PGPR samples (3 g/kg) in sugar-in-oil suspensions (650 g sugar/kg oil) are reported in Fig. 2. Data for a suspension without PGPR added are included as a reference. To assess the yield stress reducing efficacy for each PGPR (Equation (3)), the Herschel-Bulkley (H–B) yield stress was obtained by fitting Equation (2) to the experimental data. Following a suggestion in literature, only data points recorded between 0.1 and 100 1/s were included to limit the inclusion of data that may be affected by wall slip (De Graef, Depypere, Minnaert, & Dewettinck, 2011). Table 1 shows the mean Herschel-Bulkley (H–B) yield stress values and the yield stress reduction by each PGPR in relation to the mean H–B yield stress of the reference suspension, which was 57.6 ± 15.8 Pa. The

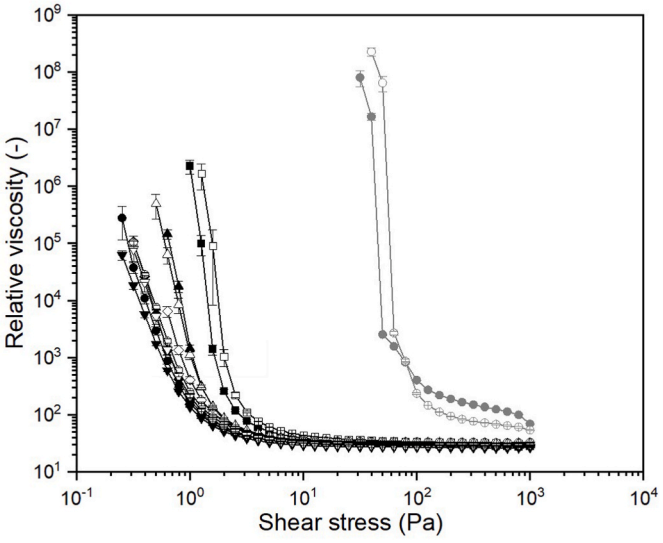

Fig. 2. Flow curves for 650 g/kg icing sugar-in-sunflower oil suspensions without and with polyglycerol polyricinoleate (PGPR) at 3 g/kg addition. The filled and open symbols refer to data acquired on two independently prepared sample batches, with three replicate measurements per batch. The error bars represent ± one standard deviation around the mean and are sometimes within the symbol. The Herschel-Bulkley model was used to calculate the yield stress; the model was fitted between 0.1 and 100 1/s to limit the inclusion of slip errors. The relative viscosity was calculated by dividing the absolute viscosity measured by the measured viscosity of treated sunflower oil in order to negate any effects of the viscosity of the continuous phase. The viscosity of treated sunflower oil was 62.8 mPa s and the viscosity of sunflower oil with the PGPR addition was 61.0 mPa s. The symbols identify the PGPR that the suspension contains: ● ○ No PGPR, ● ○ PGPR-1, ◆ ◇ PGPR-2, ■ □ PGPR-3, ▲ △ PGPR-4, ▼ ▽ PGPR-5.

Table 1
The mean Herschel-Bulkley (H–B) yield stress values of 3 g/kg polyglycerol polyricinoleate (PGPR) applied in a 650 g/kg icing sugar in sunflower oil suspension (the oil was pre-treated to remove naturally-occurring surface-active material). Values with different superscript letters differ significantly ($p < 0.05$). n is the number of replicates (three replicates from two separate batches), and the yield stress reduction is calculated using Equation (2), with $\tau_{HB,ref}$ as 57.6 Pa, the H–B yield stress of the suspension without PGPR.

PGPR	n	H–B yield stress (Pa)	Variance	Standard deviation	Yield stress reduction (%)
PGPR-1	6	0.93[c]	0.01	0.07	98.39
PGPR-2	6	1.00[c]	0.01	0.08	98.26
PGPR-3	6	1.93[a]	0.04	0.20	96.65
PGPR-4	6	1.26[b]	0.00	0.02	97.81
PGPR-5	6	0.92[c]	0.01	0.09	98.40
Pooled estimators: n = 30			**0.01**	**0.11**	

Herschel-Bulkley parameters and the quality of fit for the individual data sets are reported in Table S2.

The suspensions containing PGPR-1, -2 or -5 had the lowest H–B yield stress values. One-way ANOVA followed by a Tukey post-hoc test showed that they were not significantly different from each other ($p = 0.68$; reference suspension excluded from statistical analysis). The suspension containing PGPR-4 had a significantly higher H–B yield stress, and the suspension containing PGPR-3 had the highest H–B yield stress overall (excluding the reference sample) ($p < 0.05$). The observed variation in yield stress confirms anecdotal knowledge of variation in yield stress reducing performance among commercial PGPR samples.

3.2. Critical micelle concentration and interfacial area per molecule

Equilibrium interfacial tension data were acquired on the five PGPR samples, each dissolved in treated sunflower oil at concentrations of 0.2–50 g/kg. The results reported as interfacial tension isotherms in Fig. 3 were subsequently analysed for their critical micelle concentration (CMC) and interfacial area per molecule. As expected, interfacial tension initially decreased with an increasing concentration of PGPR, followed by a constant value at higher concentrations. The intercept of the regression lines for the two regions, see Table S3 for the fit parameters, corresponds to the CMC data reported in Fig. 4. The projected interfacial area occupied per PGPR molecule data was obtained by applying Equation (4) to the regression line in the region of decreasing interfacial tension, followed by inserting the resulting interfacial excess data into Equation (5). The data is reported alongside the CMC data in Fig. 4.

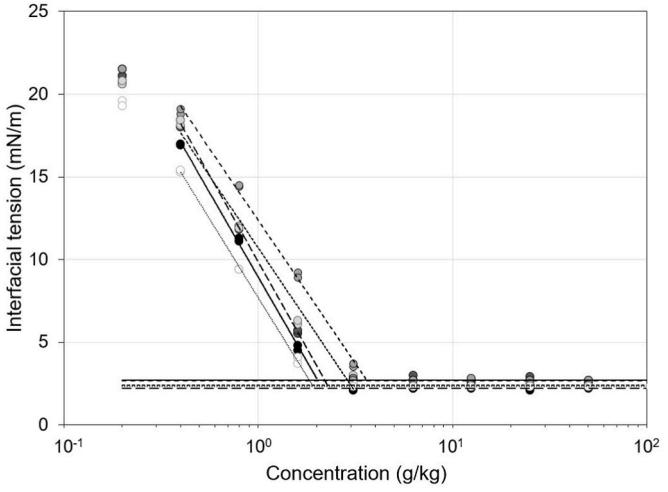

Fig. 3. The equilibrium interfacial tension values plotted against the log of the concentration of the polyglycerol polyricinoleate (PGPR) samples. Values were obtained in duplicate, and both points were used to create the trendlines. For values below the critical micelle concentration, the regression lines fit with a good correlation of R^2 higher than 0.98 for all data sets: the trendline data is shown in Table S3. The symbols and lines identify the PGPR: ● —— PGPR-1, ◐ — — — PGPR-2, ◐ - - - - PGPR-3, ◐ ------- PGPR-4, ○ ····· PGPR-5.

Fig. 4 reveals an almost perfect linear correlation between CMC and H–B yield stress ($y = 1.89x+0.54$, $r = 0.96$ ($p < 0.01$)), in the narrow value range reported for both parameters meaning that CMC is inversely correlated to yield stress reducing efficacy in this range. CMC is linked to molecular structure, and, while there is some debate in the literature on whether PGPR can form reverse micelles (Choi, Decker, Henson, Popplewell, & McClements, 2010; Nadin, Rousseau, & Ghosh, 2014; Pawlik, Cox, & Norton, 2010; Vernier, 1997; Yi et al., 2015), the following discussion leans on PGPR forming structures in which the hydrophilic heads are buried inside inverse micelle-like structures with hydrophobic tails pointing outwards at concentrations above the CMC. Considering the molecular architecture of the PGPR headgroup, a polyglycerol, we argue that a lower concentration of molecules is needed for an inverse micelle of PGPR to form if it has a larger number of glycerol sub-units. In the case of chocolate, a PGPR with a larger hydrophilic headgroup (and a lower CMC value) would interact more strongly with the hydrophilic sugar surface and thereby reduce yield stress more effectively than a PGPR with a smaller headgroup (and a higher CMC value). It has previously been shown, by comparing synthetic emulsifiers that have a similar structure to PGPR but with different headgroups, that strong, assumed to be via hydrogen bonding, headgroup interaction of emulsifiers with sugar surfaces is crucial for effective yield stress reduction

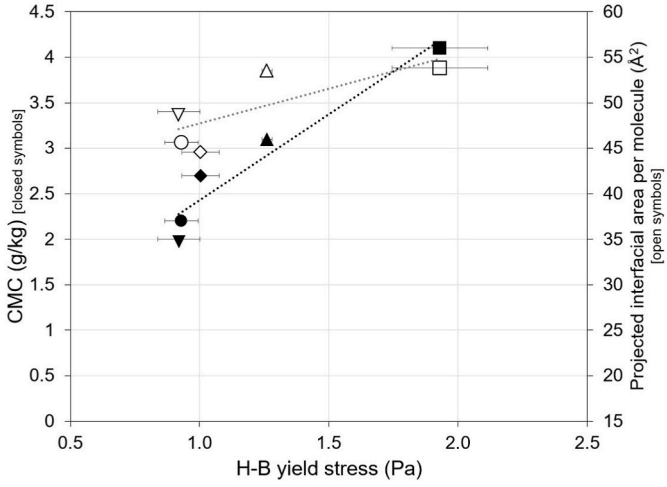

Fig. 4. Critical micelle concentration (CMC) and projected interfacial area per molecule values plotted against the mean Herschel-Bulkley (H–B) yield stress. Closed symbols show the CMC values and open symbols the projected interfacial area per molecule. Error bars have been applied to the H–B yield stress values, they represent the values' standard deviation from the mean. The CMC is determined from the intercept of the regression lines calculated from the interfacial tension measurements (Fig. 3) and interfacial area per molecule from the slope of the interfacial tension isotherms in the decreasing interfacial tension region (Fig. 3), so error bars cannot be applied. The regression line equation for CMC vs H–B yield stress data is $y = 1.89x + 0.05$, $r = 0.96$ ($p < 0.01$) and the regression line equation for the projected interfacial area per molecule vs H–B yield stress data is $y = 7.66x + 40.05$, $r = 0.76$ (p = NS) (Pearson product-moment correlation). The symbols identify the PGPR: ● ○ PGPR-1, ◆ ◇ PGPR-2, ■ □ PGPR-3, ▲ △ PGPR-4, ▼ ▽ PGPR-5.

(Vernier, 1997).

The projected interfacial area per molecule data, shown in Table 2 and included in Fig. 4), and the H–B yield stress show a non-significant correlation($y = 7.66x+40.05$, $r = 0.76$ (p = NS)). The projected interfacial area of the two least performing PGPR samples was larger than for the three other PGPR samples. If the hypothesis discussed for the CMC vs H–B yield stress finding holds, then the size difference found here must be related to the hydrophobic part of the molecule, the polyricinoleate chains, rather than the headgroup.

To validate our hypotheses regarding molecular architecture based on the data discussed thus far, a range of molecular analysis methods were applied, and the results are reported in the following.

3.3. Molecular weight range and polyricinoleate chain length

The molecular weight range (MWR) of the PGPR samples was analysed with electrospray ionisation-mass spectroscopy (ESI-MS), and the results are reported in Fig. 5. Visual inspection reveals that the MWRs of the PGPRs were very similar but skewed to the lower end of MW previously noted in literature (Dedinaite & Campbell, 2000; Orfanakis et al., 2012). The peak at 544 m/z was analysed by tandem-MS and showed no larger fragments, indicating that the molecules were not double charged; therefore, in this case, m/z is indeed equivalent to g/mol. The spectra show a two-peak, three-peak, three-peak, three-peak repeating pattern at 526–751 m/z, then more clearly at 807–1031 and 1087–1311 m/z, which can be related to the expected molecular weights of ionised PGPR molecules, see Fig. 6. Therefore, this analysis shows complete, ionised PGPR molecules rather than random fragments but at the lower end of the weight range expected. However, the ESI-MS samples were turbid, implying that not all molecules dissolved in the solvent mixture. Therefore, size-exclusion chromatography (SEC) and nuclear magnetic resonance (NMR) methods were applied to the PGPR samples as different approaches to molecular weight measurement. SEC is a method that separates molecules dissolved in a solvent based on their size. The MWR is calculated using a standard mixture of known molecule sizes, run under the same conditions as the samples. The SEC results (Fig. S1) confirmed that all five PGPRs had a very similar MWR. NMR was employed as the resonance caused by the double bonds in the polyricinoleate would be more or less pronounced depending on the number of ricinoleic acids in the estolide. The resonance in the alkene region for PGPR-3 and PGPR-5, the least and the most efficient of the five PGPR samples at lowering the yield stress, respectively, were virtually identical, as shown in Fig. S2. Therefore, the efforts of MWR analysis failed to explain the observed differences in yield stress functionality.

3.4. Fatty acid composition at the end of the polyricinoleate chains

As the MWRs were indistinguishable between the five PGPR samples, the results of an attempt to evaluate the fatty acid composition of the polyricinoleate chains using transmethylation with TMSH followed by GC-MS analysis are shown in Table 3. The TMSH reaction is mild (El-Hamdy & Christie, 1993), and the terminal or capping fatty acid of an estolide is most vulnerable to hydrolysis (Isbell, Edgcomb, & Lowery, 2001). Therefore, the fatty acids revealed by the GC-MS can be assumed to be solely the capping fatty acids of the PGPR molecules. Ricinoleic, stearic, oleic and linoleic acids were expected (Wilson et al., 1998), as well as small amounts of other fatty acids (Christiansen, 2015). In all the PGPR samples analysed, palmitic, stearic, oleic, linoleic and α-linolenic acids were identified, along with two other C18:2 peaks that elute after α-linolenic acid. This position is not normal for linoleic acid. The reason for the presence of these unusual molecules could be that they are Δ5 linoleic acid molecules which elute at a later retention time than standard linoleic acid (Wolff et al., 1999), or they could be C18:2 molecules with double bonds at different locations than a standard linoleate formed from ricinoleate due to side reactions occurring during the manufacture of the polyricinoleate chains (Wilson et al., 1998). Alternatively, it could be that the TMSH reaction has caused the formation of methoxy-FAMEs at the hydroxyl groups of ricinoleic acid during transesterification (Vosmann, Schulte, Klein, & Weber, 1998), or they may merely be isomers of linoleic acid formed because of the double bonds' rearrangement due to conjugation. The mass spectrographs do not provide a certain answer to these two peaks' identities.

Table 2
The projected area each type of polyglycerol polyricinoleate (PGPR) molecule occupies at the oil/water interface, estimated using the Gibbs Adsorption Isotherm equation applied to the decreasing interfacial tension regression lines in Fig. 3, with line fit parameters shown in Table S3.

PGPR	Area (Å^2/molecule)
PGPR-1	45.63
PGPR-2	44.54
PGPR-3	53.82
PGPR-4	53.51
PGPR-5	49.02

The most pertinent finding for this research was that PGPR-3 had significantly more ricinoleic acid acting as the capping group than the other PGPRs (38.3 mg/g PGPR compared with the next highest, which was PGPR-2 with 27.2 mg/g PGPR). As PGPR-3 was the least efficacious at reducing the yield stress, this is an important finding. The hydroxyl group on the ricinoleate at the end of the chain makes it more hydrophilic, so it may be that the chain folds back and adsorbs at the sugar surface. Thus, the effective length of the polyricinoleate chain extending into the oil phase and contributing to yield stress reduction is compromised. Equally, such folding back would explain the higher area per molecule value (Table 2) found for PGPR-3 compared to the PGPR-1, -2 and -5, which could not be explained by considering the hydrophilic headgroup of this molecule alone. For PGPR-4, there was no specific insight; however, it could be that the hydrophobic molecules were more branched, leading to the increased projected interfacial area per molecule value, if it is indeed true that the hydrophilic headgroup size in these systems is inversely correlated to CMC in general (Fig. 4).

The idea of molecular folding can also be applied to the pillow model of PGPR functionality discussed by Middendorf et al. (2015); folding back leads to thinner pillows. A schematic of our proposition of how the more hydrophilic end caps contribute to PGPR molecular arrangements at or near a hydrophilic sugar surface is presented in Fig. 7.

4. Conclusions

All five commercial PGPRs assessed in this research were of a similar molecular weight range but differed in the number of ricinoleate capping fatty acids at the end of the hydrophobic chains. Ricinoleate would impart a hydrophilic character to the end of the chain, and we propose that the hydroxyl group may interact with the sugar surface, thereby reducing the efficacy of the PGPR. It was found that critical micelle concentration and yield stress were strongly correlated indicating that the interaction at the sugar surface is important for superior yield stress reduction; however, this result should not be over-interpreted due to the narrow value range of both parameters. The interfacial area data revealed that molecular architecture features of the hydrophobic molecule part of PGPR, which were not uncovered in this study, might also lead to poor performance in terms of yield stress reduction. However, it can be concluded that, in the search for an alternative to PGPR, an amphiphile with a poly-fatty acid tail containing no hydrophilic regions and possibly a large hydrophilic head group would be a prime candidate. PGPR is used in applications other than in chocolate, such as margarine, spreads and dressing, as it readily forms water-in-oil emulsions (Garti, Binyamin, & Aserin, 1998). It could be conceived that the findings of this research could be transferred into

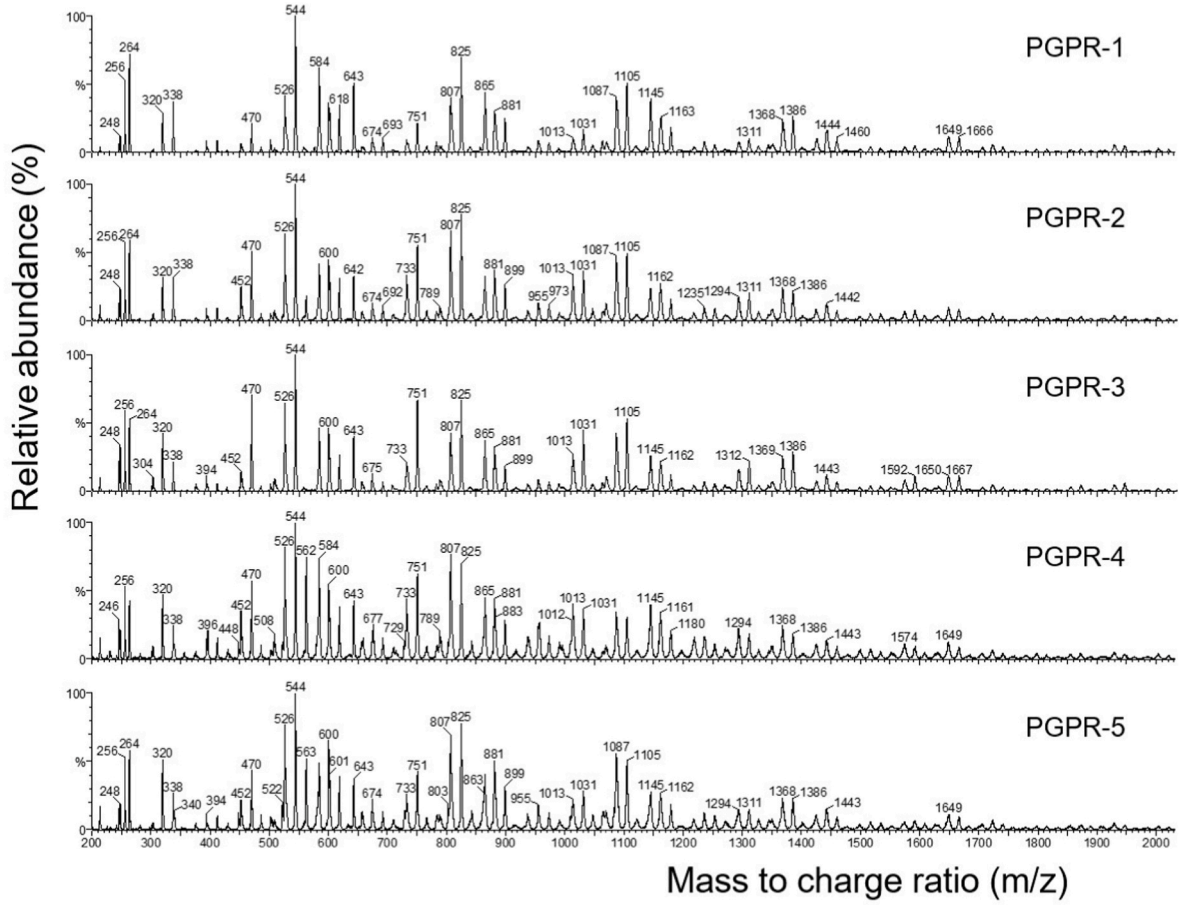

Fig. 5. Spectra from all polyglycerol polyricinoleates (PGPRs) samples obtained using electrospray ionisation-mass spectrometry. The spectra are very similar, with a curve skewed to the left, ranging from 200 to 2000 m/z. The most abundant peak for all PGPRs was at 544 m/z.

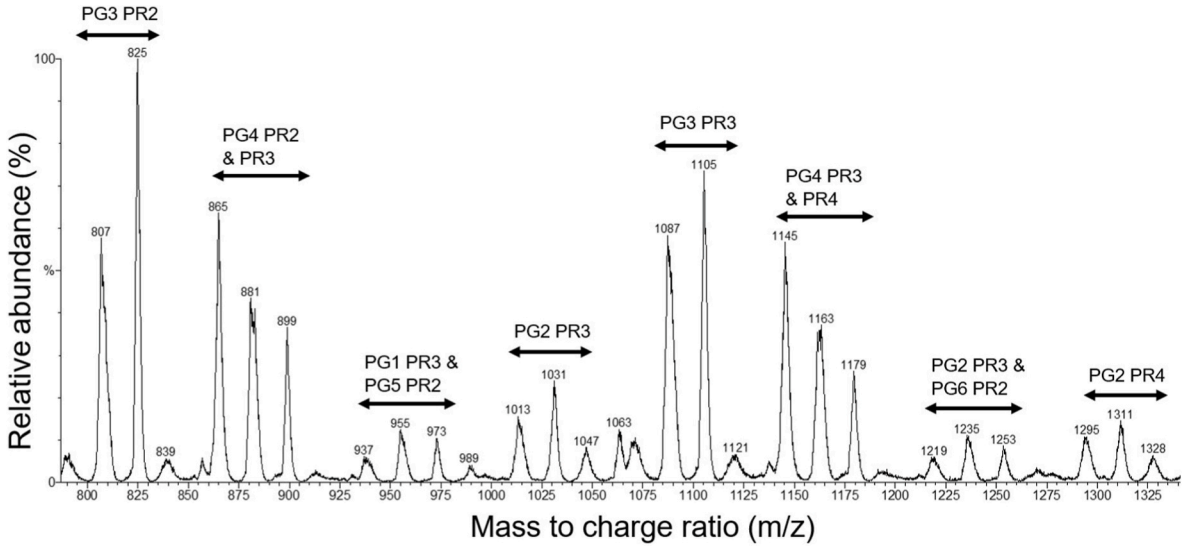

Fig. 6. The spectrum shown in Fig. 5 but focused on 775–1350 m/z (PG = a number of glycerol units linked together with ether bonds, PR = a number of ricinoleate units linked together with ester bonds. The numeral following the code denotes the number of units in that molecule).

these contexts.

Declaration of competing interest

The authors declare that they have no conflicts of interest.

CRediT authorship contribution statement

Ruth Price: Methodology, Investigation, Formal analysis, Writing – original draft, preparation. **David Gray:** Conceptualization, Supervision, Writing – review & editing. **Nicholas Watson:** Supervision,

Table 3
The fatty acids, given as mg of fatty acid per g of polyglycerol polyricinoleate sample, that are located at the end of the polyricinoleate estolides, measured using a gas chromatograph-mass spectrometer after transesterification of the polyglycerol polyricinoleate molecules. Different lower-case letters in superscript indicate significant differences within each fatty acid type ($p < 0.05$). n is the number of replicates (three aliquots processed separately from each sample of PGPR). The variances and pooled variances are given in brackets.

	n	C16:0 Palmitate	C18:0 Stearate	C18:1 Oleate	C18:2 Linoleate	C18:3 α-Linoleate	C18:2	C18:2	C18:1 (OH) Ricinolate
PGPR-1	3	14.473 ^{a} (0.046)	15.163 ^{a} (0.082)	7.196 ^{b} (0.020)	14.960 ^{b} (0.269)	1.335 ^{b} (0.002)	7.514 ^{b} (0.899)	2.655 ^{b} (0.762)	26.007 ^{b} (2.569)
PGPR-2	3	9.288 ^{c} (0.041)	11.682 ^{c} (0.053)	6.514 ^{c} (0.016)	17.818 ^{a} (0.228)	1.141 ^{b} (0.002)	17.808 ^{a} (2.082)	5.361 ^{a} (0.969)	27.213 ^{b} (0.503)
PGPR-3	3	12.230 ^{b} (0.142)	13.287 ^{b} (0.018)	8.342 ^{a} (0.174)	17.133 ^{a} (0.019)	1.728 ^{a} (0.025)	7.336 ^{b} (4.788)	2.611 ^{b} (0.986)	38.326 ^{a} (0.664)
PGPR-4	3	9.732 ^{c} (0.085)	11.171 ^{cd} (0.043)	6.888 ^{bc} (0.040)	15.622 ^{b} (0.008)	1.298 ^{b} (0.001)	10.573 ^{b} (1.734)	2.782 ^{b} (0.086)	22.473 ^{c} (0.126)
PGPR-5	3	9.382 ^{c} (0.208)	10.656 ^{d} (0.097)	6.520 ^{c} (0.049)	15.112 ^{b} (0.002)	1.235 ^{b} (0.005)	11.008 ^{b} (2.631)	3.423 ^{ab} (0.717)	21.326 ^{c} (0.119)
Pooled variance	15	(0.104)	(0.059)	(0.060)	(0.105)	(0.007)	(2.427)	(0.704)	(0.796)

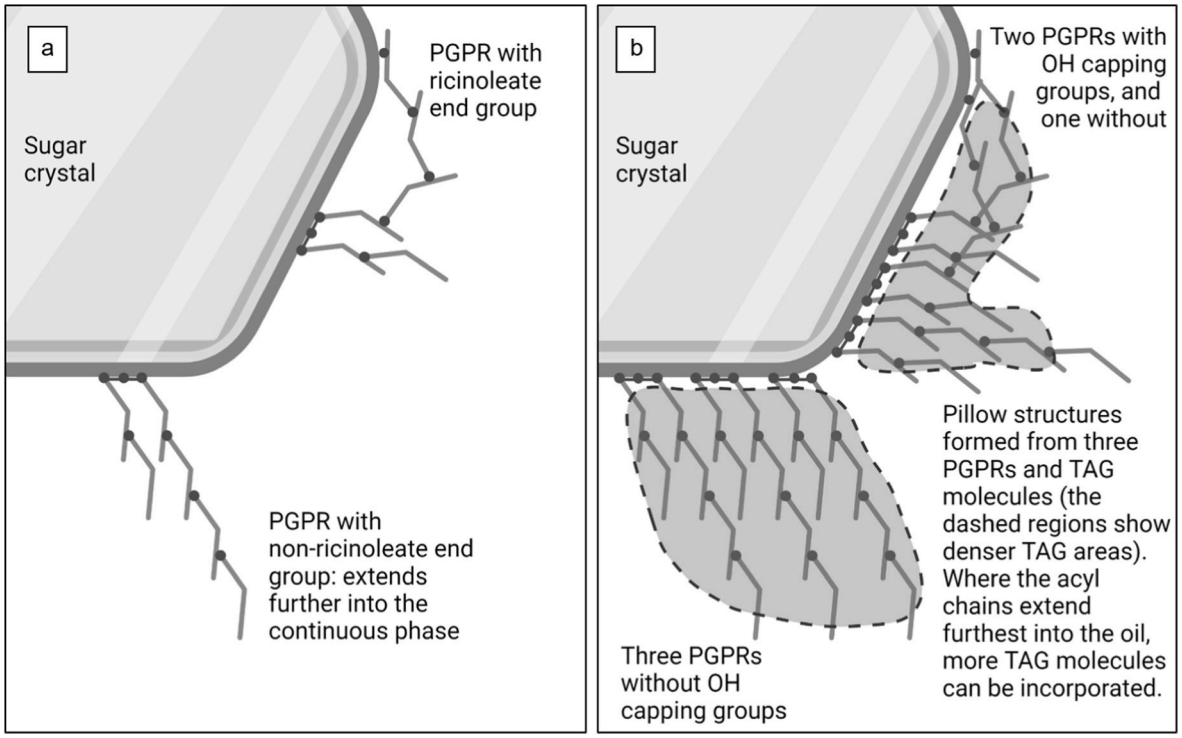

Fig. 7. Illustrations to describe the possible result of a hydroxyl group on the end fatty acid of the polyricinoleate chain, using the traditional adsorption theory (a) and the pillow theory (b) (drawn with BioRender).

Writing – review & editing. **Josélio Vieira:** Conceptualization, Supervision, Resources, Writing – review & editing. **Bettina Wolf:** Conceptualization, Supervision, Funding acquisition, Writing – review & editing.

Acknowledgements

We are grateful to the BBSRC (grant number RT3515) and Nestlé for supplying the funding for this research. We would also like to thank Elaine Andrews and her team at Nestlé for performing the particle size analysis on the sugar sample, Dr Daniel W. Lester in the Polymer Characterisation Research Technology Platform at the University of Warwick for performing the SEC experiments and Dr Huw E. L. Williams at the Centre for Biomedical Sciences at the University of Nottingham who performed the NMR experiments.

Appendix A. Supplementary data

Supplementary data to this article can be found online at https://doi.org/10.1016/j.lwt.2022.113704.

References

Bahrami, N., Yonekura, L., Linforth, R., Carvalho Da Silva, M., Hill, S., Penson, S., et al. (2014). Comparison of ambient solvent extraction methods for the analysis of fatty acids in non-starch lipids of flour and starch. *Journal of the Science of Food and Agriculture, 94*, 415–423.

Bamford, H. F., Gardner, K. J., Howat, G. R., & Thomson, A. F. (1970). The use of polyglycerol polyricinoleate in chocolate. *Revue International de la Chocolaterie, 25*, 226–228.

Bastida-Rodríguez, J. (2013). *The food additive polyglycerol polyricinoleate (E-476): Structure, applications, and production methods* (pp. 1–21). ISRN Chemical Engineering, 2013.

Beckett, S. T. (2019). *The science of chocolate* (3rd ed., Vol. 284). Croyden, UK: The Royal Society of Chemistry, ISBN 978-1-78801-235-5.

CEC. (2008). Commission Directive 2008/84/EC of 27 August 2008 laying down specific purity criteria on food additives other than colours and sweeteners. *Official Journal of the European Union L, 253*, 109–110.
Choi, S. J., Decker, E. A., Henson, L., Popplewell, L. M., & McClements, D. J. (2010). Inhibition of citral degradation in model beverage emulsions using micelles and reverse micelles. *Food Chemistry, 122*, 111–116.
Christiansen, K. (2015). PGPR, polyglycerolpolyricinoleate, E476. In V. Norn (Ed.), *Emulsifiers in food Technology* (2nd ed., pp. 209–229). Chichester, UK: John Wiley & Sons, Ltd.
Crapiste, G. H., Brevedan, M. I., & Carelli, A. A. (1999). Oxidation of sunflower oil during storage. *Journal of the American Oil Chemists' Society, 76*, 1437.
De Graef, V., Depypere, F., Minnaert, M., & Dewettinck, K. (2011). Chocolate yield stress as measured by oscillatory rheology. *Food Research International, 44*, 2660–2665.
Dedinaite, A., & Campbell, B. (2000). Interactions between mica surfaces across triglyceride solution containing phospholipid and polyglycerol polyricinoleate. *Langmuir, 16*, 2248–2253.
El-Hamdy, A., & Christie, W. (1993). Preparation of methyl esters of fatty acids with trimethylsulphonium hydroxide—an appraisal. *Journal of Chromatography A, 630*, 438–441.
FCC. (2016). *Food Chemicals Codex, United States pharmacopeial convention*.
Garti, N., Binyamin, H., & Aserin, A. (1998). Stabilisation of water-in-oil emulsions by submicrocrystalline α-form fat particles. *Journal of the American Oil Chemists' Society, 75*, 1825–1831.
Gonçalves, E. V., & Lannes, S. C. D. S. (2010). Chocolate rheology. *Food Science and Technology, 30*, 845–851.
Gould, J. M., Furse, S., & Wolf, B. (2016). The role of endogenous lipids in the emulsifying properties of cocoa. *Frontiers of Chemistry, 4*, 11.
Isbell, T. A. (2011). Chemistry and physical properties of estolides. *Grasas Y Aceites, 62*, 8–20.
Isbell, T. A., Edgcomb, M. R., & Lowery, B. A. (2001). Physical properties of estolides and their ester derivatives. *Industrial Crops and Products, 13*, 11–20.
JECFA. (1992). *Joint FAO/WHO expert committee on food additives: Compendium of food additive specifications*. Rome: Food and Agriculture Organization of the United Nations.
Johansson, D., & Bergenståhl, B. (1992a). The influence of food emulsifiers on fat and sugar dispersions in oils. I. Adsorption, sedimentation. *Journal of the American Oil Chemists Society, 69*, 705–717.
Johansson, D., & Bergenståhl, B. (1992b). The influence of food emulsifiers on fat and sugar dispersions in oils. II. Rheology, colloidal forces. *Journal of the American Oil Chemists' Society, 69*, 718–727.
Kamphuis, H. J. (2017). Sugar and bulk sweeteners. In S. T. Beckett, M. S. Fowler, & G. R. Zielger (Eds.), *Industrial chocolate manufacture and use* (pp. 72–101). Chichester, UK: Blackwell Publishing Ltd.
Middendorf, D., Juadjur, A., Bindrich, U., & Mischnick, P. (2015). AFM approach to study the function of PGPR's emulsifying properties in cocoa butter based suspensions. *Food Structure, 4*, 16–26.
Nadin, M., Rousseau, D., & Ghosh, S. (2014). Fat crystal-stabilised water-in-oil emulsions as controlled release systems. *LWT - Food Science and Technology, 56*, 248–255.
Orfanakis, A., Hatzakis, E., Kanaki, K., Pergantis, S. A., Rizos, A., & Dais, P. (2012). Characterisation of polyglycerol polyricinoleate formulations using NMR spectroscopy, mass spectrometry and dynamic light scattering. *Journal of the American Oil Chemists' Society, 90*, 39–51.
Osborn, S. (2015). Labelling relating to natural ingredients and additives. In P. Berryman (Ed.), *Advances in Food and beverage labelling: Information and regulations* (pp. 207–221). Elsevier Ltd. https://doi.org/10.1533/9781782420934.3.207.
Pawlik, A., Cox, P. W., & Norton, I. T. (2010). Food grade duplex emulsions designed and stabilised with different osmotic pressures. *Journal of Colloid and Interface Science, 352*, 59–67.
Rector, D. (2000). Chocolate-controlling the flow. *The Manufacturing Confectioner, 80*, 63–70.
Vernier, F. C. (1997). *Influence of emulsifiers on the rheology of chocolate and suspensions of cocoa or sugar particles in oil. PhD*. The University of Reading.
Vosmann, K., Schulte, E., Klein, E., & Weber, N. (1998). Formation of N-and O-methyl derivatives of lipids containing amino, amide or hydroxy groups by the pyrolytic reaction with trimethylsulfonium hydroxide. *European Journal of Lipid Science and Technology, 100*, 334–342.
Wilson, R., Van Schie, B., & Howes, D. (1998). Overview of the preparation, use and biological studies on polyglycerol polyricinoleate (PGPR). *Food and Chemical Toxicology, 36*, 711–718.
Wolff, R. L., Christie, W. W., Pedrono, F., Marpeau, A. M., Tsevegsuren, N., Aitzetmuller, K., et al. (1999). Delta5-olefinic acids in the seed lipids from four Ephedra species and their distribution between the alpha and beta positions of triacylglycerols. Characteristics common to coniferophytes and cycadophytes. *Lipids, 34*, 855–864.
Yi, J., Dong, W., Zhu, Z., Liu, N., Ding, Y., Mcclements, D. J., et al. (2015). Surfactant concentration, antioxidants, and chelators influencing oxidative stability of water-in-walnut oil emulsions. *Journal of the American Oil Chemists' Society, 92*, 1093–1102.
Zerkowski, J. A. (2008). Estolides: From structure and function to structured and functionalised. *Lipid Technology, 20*, 253–256.
Ziegler, G. R., & Hogg, R. (2017). Particle size reduction. In S. T. Beckett, M. S. Fowler, & G. R. Zielger (Eds.), *Industrial chocolate manufacture and use* (pp. 216–240). Chichester, UK: Blackwell Publishing Ltd.